Proceedings of the 26th Chinese Control Conference
July 26-31, 2007, Zhangjiajie, Hunan, China

# Tracking of Nonholonomic Control Systems Based on Visual Servoing Feedback *

Li Qingsong, Wang Chaoli, Niu Wenbin
Electric Engineering College, University of Shanghai for Science and Technology, Shanghai 200031, P. R. China
E-mail: pine5@163.com, clclwang@126.com, wbn05@tom.com

**Abstract:** This paper investigated the visual servoing tracking of nonholonomic mobile robots. Nonholonomic kinematic systems with visual feedback are uncertain and more involved in comparison with common kinematic systems. Barbalat theorem and two-step techniques were exploited to craft a robust controller that enables the mobile robot image pose and the orientation tracking despite the lack of depth information and the lack of precise visual parameters. The most interesting feature of this paper is that the problem was discussed in the image frame and the inertial frame, which made the problem easy and useful. The convergence of the error system by using the proposed method was rigorously proved. The simulation was given to show the effectiveness of the presented controllers.

**Key Words:** Tracking, Nonholonomic, Visual Servoing, Robot

## 1 INTRODUCTION

Mobile robot is one of the well-known systems with nonholonomic constraints [1, 2]. By the theorem of R. Brockett(1983) [3], a nonholonomic system cannot be stabilized at a single equilibrium point by a smooth feedback controller. To solve this problem, lots of methods have been considered, such as chained form methods [4, 5], tracking control [6] and discontinuous feedback control [7] etc. In the control of nonholonomic mobile robots, it is usually assumed that the robot states are available and exactly reconstructed using proprioceptive and exteroceptive sensor measurements. But in practical mobile robot applications, there are several ideal conditions that can not be satisfied, such as uncertainties in the kinematic model, mechanical limitations, noise and so on. The estimation of the robot state from sensor measurements can be affected by these perturbations. Visual feedback is an important approach to improve the control performance of manipulators since it mimics the human sense of vision and allows for operating on the basis of noncontact measurement and unconstructure of the environment. Since the late 1980s, tremendous effort has been made to visual servoing and vision-based manipulations [8].

The nonholonomic control problem results to be more involved because of the visual feedback. Designing the feedback at the sensor level increases system performances especially when uncertainties and disturbances affect the robot model and the camera calibration, see [9] and therein references.

Based on the success of image extraction/interpretation technology and advances in control theory, research has focused on the use of monocular camera-based vision systems for navigating a mobile robot [10]. A significant issue with monocular camera-based vision systems is the lack of depth information. From a review of literature, various approaches have been developed to address the lack of depth information inherent in monocular vision systems. For example, using consecutive image frames and an object database, Kim et al [11]. recently proposed a mobile robot tracking controller based on a monocular visual feedback strategy. To achieve their result, they linearized the system equations using a Taylor series approximation, and then applied extended Kalman filtering (EKF) techniques to compensate for the lack of depth information [11]. Dixon et al [12]. used feedback from an uncalibrated, fixed (ceiling-mounted) camera to develop an adaptive tracking controller for a mobile robot that compensated for the parametric uncertainty in the camera and the mobile robot dynamics. Dixon et al. exploit Lyapunov-based adaptive techniques to compensate for the unknown depth information [12]. However, to employ these techniques, they require the depth from the camera to the mobile robot plane of motion to remain constant (i.e., the camera plane and the mobile robot plane must be parallel). This assumption reduces the nonlinear pinhole camera model to a decoupled linear transformation; however, it also restricts the applicability of the controller. Wang et al [13]. also exploit a Lyapunov-based adaptive technique to compensate for a constant unknown depth parameter for a monocular mobile robot tracking problem. While the approach in [13] may be well suited for tracking applications, the stability analysis requires the same restrictions on the reference trajectory of the mobile robot as in [12], and hence, cannot be applied to solve the regulation problem.

The contribution of this paper is that the tracking problem was formulated in the image frame and the inertial frame. This made the problem easy and simple. Barbalat theorem and two-step techniques were exploited to craft a robust controller that enables the mobile robot image pose and the orientation tracking despite the lack of depth information and the lack of precise visual parameters provided that the camera plane and the mobile robot plane must be parallel. Due to assumptions on the reference trajectory resulting from the nonholonomic constraint, the aforementioned visual servo tracking control results cannot be applied to solve the regulation problem considered in the current result. The result in this paper is achieved with a monocular vision system with uncalibrated visual parameters, and the control design approach incorporates the full nonholonomic kinematic equa-

* This paper was supported by The National Nature Science Foundation(60474009), Shu Guang Program(05SG48) and The Development Foundation of Shanghai Education Committee.

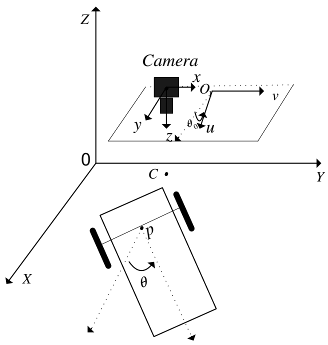

**Fig. 1 Wheeled Mobile Robots with Monocular Camera**

tions of motion.

The paper is organized as follows. Section 2 introduces the camera-object visual model in terms of the planar optical flow equations. In Section 3, the controllers are synthesized for several cases. In Section 4, the simulation results carried out to validate the theoretical framework. Finally, in Section 5 the major contribution of the paper is summarized.

## 2 PROBLEM STATEMENT

### 2.1 System Configuration

In the Fig.1 of the mobile robot shown below. Assume that a pinhole camera is fixed to the ceiling and the camera plane and the mobile robot plane are parallel. There are three coordinate frames, namely the inertial frame $X-Y-Z$, the camera frame $x-y-z$ and the image frame $u-O_1-v$. Assume that the $x-y$ plane of the camera frame is the identical one with the plane of the image coordinate plane. $C$ is the crossing point between the optical axis of the camera and $X-Y$ plane. Its coordinate relative to $X-Y$ plane is $(p_x,p_y)$, the coordinate of the original point of the camera frame with respect to the image frame is defined by $(O_{c1},O_{c2})$, $(x,y)$ is the coordinate of the mass center of the robot with respective to $X-Y$ plane. Suppose that $(x_m,y_m)$ is the coordinate of $(x,y)$ relative to the image frame. Pinhole camera model yields

$$\begin{bmatrix} x_m \\ y_m \end{bmatrix} = \begin{bmatrix} \alpha_1 & 0 \\ 0 & \alpha_2 \end{bmatrix} R \left[ \begin{bmatrix} x \\ y \end{bmatrix} - \begin{bmatrix} p_x \\ p_y \end{bmatrix} \right] + \begin{bmatrix} O_{c1} \\ O_{c2} \end{bmatrix} \tag{1}$$

where $\alpha_1,\alpha_2$ are constant which are dependent on the depth formation, focus length, scalar factors along $x$ axis and $y$ axis respectively.

$$R = \begin{bmatrix} \cos\theta_0 & \sin\theta_0 \\ -\sin\theta_0 & \cos\theta_0 \end{bmatrix} \tag{2}$$

where $\theta_0$ denotes the angle between $u$ axis and $X$ axis with a positive anticlockwise orientation.

### 2.2 Problem Description

Assume that the geometric center point and the mass center point of the robot are the same. The nonholonomic constraint is defined by

$$\dot{x}\sin\theta - \dot{y}\cos\theta = 0 \tag{3}$$

By this formula, nonholonomic kinematic equation is written by

$$\begin{cases} \dot{x} = v\cos\theta \\ \dot{y} = v\sin\theta \\ \dot{\theta} = \omega \end{cases} \tag{4}$$

where $v$ and $\omega$ denote the velocity of the heading direction of the robot and the angle velocity of the rotation of the robot, respectively.

In the image frame, the kinematic model can be deduced by (1)

$$\begin{aligned} \begin{bmatrix} \dot{x}_m \\ \dot{y}_m \end{bmatrix} &= \begin{bmatrix} \alpha_1 & 0 \\ 0 & \alpha_2 \end{bmatrix} R \begin{bmatrix} \dot{x} \\ \dot{y} \end{bmatrix} \\ &= \begin{bmatrix} \alpha_1 & 0 \\ 0 & \alpha_2 \end{bmatrix} R v \begin{bmatrix} \cos\theta \\ \sin\theta \end{bmatrix} \\ &= v \begin{bmatrix} \alpha_1\cos(\theta-\theta_0) \\ \alpha_2\sin(\theta-\theta_0) \end{bmatrix} \end{aligned} \tag{5}$$

Generally, $(x,y)$ can be obtained from the encoders of motors and other sensors such as ultrasonic sensors, infrared sensors, etc.. However, for complex environment, it is difficult to do it. But vision information can be easily exploited to deal with this problem.

In this paper, the camera is used to measure $(x,y)$ and determine the desired target. A kind of effective method is that the error between the mass center point of the robot and its desired point in the image frame can be used in the closed-loop feedback control of the robot. As for the angle, $\theta$, it can be obtained easily from the angle sensor. Therefore, $\theta$ is still included in the error model.

From (5), the regulation problem can be described by

$$\begin{bmatrix} \dot{x}_m \\ \dot{y}_m \\ \dot{\theta} \end{bmatrix} = \begin{bmatrix} v\cdot\alpha_1\cos(\theta-\theta_0) \\ v\cdot\alpha_2\sin(\theta-\theta_0) \\ \omega \end{bmatrix} \tag{6}$$

where $(x_m,y_m)$ denotes the coordinate of the robot mass center $(x,y)$ in the image frame. $\theta$ is the angular between the forward direction of the robot and the inertia frame. $v$ and $\omega$ are the forward velocity and the angular velocity of the practical robot, respectively. $\alpha_1$ and $\alpha_2$ are the scalar factors of the camera along $x$-axis and $y$-axis, respectively. $\theta_0$ denotes the angular between the two $x$-axis of the inertial frame and the image frame.

In order to discuss the tracking problem of the system (6), the desired path is given by

$$\begin{bmatrix} \dot{x}_r \\ \dot{y}_r \\ \dot{\theta}_r \end{bmatrix} = \begin{bmatrix} v_r\cdot\alpha_1\cos(\theta_r-\theta_0) \\ v_r\cdot\alpha_2\sin(\theta_r-\theta_0) \\ \omega_r \end{bmatrix} \tag{7}$$

where $(x_r,y_r)$ is the desired path of the mass center $(x,y)$ in the image frame, $\theta_r$ is the desired direction. $v_r$ and $\omega_r$ are the desired forward velocity and the desired angular velocity of the desired robot, respectively.

**Assumption 1** $v_r$, $\omega_r$ and their derivatives are bounded.

Compared with the normal nonholonomic kinematic control systems, it can be regarded as a special case where $\alpha_1 = \alpha_2 = 1$, $\theta_0 = 0$ in (6). However, for visual sensors, it is not practical. Usually, if $\alpha_1$, $\alpha_2$ and $\theta_0$ are known, it can be reduced a normal form by using coordinate transformation.

Take the transformation defined as

$$\begin{bmatrix} z_1 \\ z_2 \end{bmatrix} = \begin{bmatrix} \frac{1}{\alpha_1}\cos\theta_0 & -\frac{1}{\alpha_2}\sin\theta_0 \\ \frac{1}{\alpha_1}\sin\theta_0 & \frac{1}{\alpha_2}\cos\theta_0 \end{bmatrix} \begin{bmatrix} x_m \\ y_m \end{bmatrix} \tag{8}$$

one reduces

$$\begin{bmatrix} \dot{z}_1 \\ \dot{z}_2 \end{bmatrix} = v\begin{bmatrix} \frac{1}{\alpha_1}\cos\theta_0 & -\frac{1}{\alpha_2}\sin\theta_0 \\ \frac{1}{\alpha_1}\sin\theta_0 & \frac{1}{\alpha_2}\cos\theta_0 \end{bmatrix} \cdot \begin{bmatrix} \alpha_1\cos(\theta-\theta_0) \\ \alpha_2\sin(\theta-\theta_0) \end{bmatrix} = \begin{bmatrix} v\cos\theta \\ -v\sin\theta \end{bmatrix} \tag{9}$$

which means

$$\begin{bmatrix} \dot{z}_1 \\ \dot{z}_2 \\ \dot{z}_3 \end{bmatrix} = \begin{bmatrix} v\cos\theta \\ v\sin\theta \\ \omega \end{bmatrix} \tag{10}$$

This is consistent with the usual nonholonomic kinematic equation of mobile robots. Their tracking problems can be addressed by lots of methods. But most assumed that $v_r(t) \nrightarrow 0$ as $t \to \infty$.

On the one hand, it will bring some unconvenience. On the other hand, in practice, $\alpha_1$, $\alpha_2$ and $\theta_0$ cannot be measured. Therefore, the transformation (8) is usually not available.

As usual, these parameters can be obtained by using calibrate methods. But too much effort on calculation must be spent for calibration. The problem considered here is how to discuss the tracking of the system without calibration.

## 3 CONTROLLER DESIGN

### 3.1 Non zero limit of the velocity of the desired robot at the infinity of time

First, consider that the convergence of $\omega_r(t)$ is not zero as $t \to \infty$ or the convergence of $v_r(t)$ is not zero as $t \to \infty$. Under this case, How is the tracking controller inverestigated for the system (10)?

Consider the tracking control problem when $\alpha_1$ and $\alpha_2$ are unknown and $\theta_0$ is known.

**Assumption 2** $\alpha_1 = \alpha_2 = \alpha$, $\underline{\alpha} \leqslant \alpha \leqslant \overline{\alpha}$ are unknown, $\underline{\alpha}$ and $\overline{\alpha}$ are known.

Take the error transformation defined as

$$\begin{bmatrix} e_1 \\ e_2 \\ e_3 \end{bmatrix} = \begin{bmatrix} \cos(\theta-\theta_0) & \sin(\theta-\theta_0) & 0 \\ -\sin(\theta-\theta_0) & \cos(\theta-\theta_0) & 0 \\ 0 & 0 & 1 \end{bmatrix} \begin{bmatrix} x_r - x_m \\ y_r - y_m \\ \theta_r - \theta \end{bmatrix} \tag{11}$$

Derivating and using (6) and (7) are

$$\begin{bmatrix} \dot{e_1} \\ \dot{e_2} \\ \dot{e_3} \end{bmatrix} = \omega \begin{bmatrix} e_2 \\ -e_1 \\ 0 \end{bmatrix} + \begin{bmatrix} -v\alpha + v_r\alpha\cos(\theta-\theta_r) \\ -v_r\alpha\sin(\theta-\theta_r) \\ \omega_r - \omega \end{bmatrix} \tag{12}$$

which means

$$\begin{cases} \dot{e_1} = e_2\omega - v\alpha + v_r\alpha\cos e_3 \\ \dot{e_2} = -e_1\omega + v_r\alpha\sin e_3 \\ \dot{e_3} = \omega_r - \omega \end{cases}$$

Now consider how to develop the controller $v$ and $\omega$ such that the states of the system defined as

$$\begin{bmatrix} \dot{e_1} \\ \dot{e_2} \\ \dot{e_3} \end{bmatrix} = \begin{bmatrix} e_2\omega - v\alpha + v_r\alpha\cos e_3 \\ -e_1\omega + v_r\alpha\sin e_3 \\ \omega_r - \omega \end{bmatrix} \tag{13}$$

$e_1$,$e_2$ and $e_3$ converge to zero as $t \to \infty$.

Take the candidate Lyapunov function of the system (13) as follows

$$V = \frac{1}{2}(e_1^2 + e_2^2 + \alpha e_3^2) \tag{14}$$

Derivating it along the system (13) results in

$$\begin{aligned} \dot{V} &= e_1(e_2\omega - v\alpha + v_r\alpha\cos e_3) \\ &\quad + e_2(-e_1\omega + v_r\alpha\sin e_3) + \alpha e_3(\omega_r - \omega) \end{aligned} \tag{15}$$

Choose the controller as follows:

$$v = k_1e_1 + v_r\cos e_3, \quad \omega_r - \omega = -k_3e_3 - \frac{e_2v_r\sin e_3}{e_3} \tag{16}$$

Substituting (16) into (15) yields

$$\dot{V} = -k_1\alpha e_1^2 - k_3\alpha e_3^2 \tag{17}$$

So $V$ is monotonously decreasing. Therefore, $e_1$,$e_2$ and $e_3$ are bounded,and $e_1 \in L_2$,$e_3 \in L_2$. By Barbalat theorem, $e_1 \to 0$ and $e_3 \to 0$ as $t \to \infty$. Substituting (16) into (13), we have

$$\begin{cases} \dot{e_1} = e_2(\omega_r + k_3e_3 + \frac{e_2v_r\sin e_3}{e_3}) - k_1e_1 \\ \dot{e_2} = -e_1(\omega_r + k_3e_3 + \frac{e_2v_r\sin e_3}{e_3}) - v_r\alpha\sin e_3 \\ \dot{e_3} = -k_3e_3 - \frac{e_2v_r\sin e_3}{e_3} \end{cases} \tag{18}$$

In order to prove the convergence of $e_2$,The extended Barbalat theorem is introduced below

**Lemma 1** *If the differentiable function $f(t)$ has a finite limit as $t \to \infty$, and $\dot{f}(t)$ can be divided into two parts, one is uniformly continuous and the other is convergent to zero as $t \to \infty$, then $\dot{f}(t) \to 0$, so is the part of the uniform continuity in $\dot{f}(t)$.*

Its proof was seen in [14].

Consider (18) by using the Lemma. Because $e_1$, $e_2$ and $e_3$ are bounded, it is easy to show that $\frac{e_2v_r\sin e_3}{e_3}$ is uniformly continuous only if $v_r$ and $\dot{v}_r$ are bounded. Because $e_3 \to 0$, using Lemma and the third equation of formula (18) result in

$$e_2v_r \to 0, \ as\ t \to \infty$$

where it is derived by utilizing $\frac{\sin e_3}{e_3} \to 1$ as $e_3 \to 0$. It is concluded that $\frac{\sin e_3}{e_3}$ is uniformly continuous in $[0, +\infty)$.

By using the result, the first formula of (18),and Lemma, one yields $e_2\omega_r \to 0$. Since $e_1 \to 0$,$e_3 \to 0$,$\omega_r$ and $v_r$ are bounded,

$$e_iv_r \to 0, \ e_i\omega_r \to 0, \ (i = 1,2\ldots n)$$

Hence

$$Vv_r \to 0, \ V\omega_r \to 0$$

It is noted that $V(t)$ is convergent. Therefore, it is certain that $v \to 0$ if one of the two convergence of $v_r$ and $\omega_r$ is not zero. Furthermore, $e_2 \to 0$. In comparison with the condition in [][] where $\omega_r \to 0$ has to be required, the condition given here is not strict. In addition, it is applicable to the case with unknown $\alpha$.

### 3.2 Zero limit of the velocity of the desired robot at the infinity of time

If $\omega_r \to 0$ and $v_r \to 0$, the above controller cannot be utilized Next consider this case.

**Step 1** Choose parameter $k, k_1$ and $k_2$ such that

$$k > 0, k_1 > 0, k_2 < \frac{k}{\overline{\alpha}} \tag{19}$$

or

$$k < 0, k_1 > 0, k_2 > -\frac{k}{\overline{\alpha}} \tag{20}$$

where $\alpha \leqslant \bar{\alpha}$. The controller is given below

$$\omega = k, v = v_r \cos e_3 + k_1 e_1 + k_2 e_2 \tag{21}$$

Substituting it into (12), consider the subsystem composed of $e_1$ and $e_2$ as following

$$\begin{cases} \dot{e_1} = e_2 k - k_1 \alpha_1 - k_2 \alpha_2 \\ \dot{e_2} = -e_1 k + v_r \alpha \sin e_3 \end{cases}$$

or

$$\begin{bmatrix} \dot{e_1} \\ \dot{e_2} \end{bmatrix} = A \begin{bmatrix} e_1 \\ e_2 \end{bmatrix} + \begin{bmatrix} 0 \\ 1 \end{bmatrix} v_r \alpha \sin e_3 \tag{22}$$

where

$$A = \begin{bmatrix} -k_1\alpha & k - k_2\alpha \\ -k & 0 \end{bmatrix}$$

Solving the characteristic polynomial of matrix $A$ yields

$$|\lambda I - A| = \begin{vmatrix} \lambda + k_1\alpha & -k + k_2\alpha \\ k & \lambda \end{vmatrix}$$

which has

$$\lambda^2 + k_1\alpha\lambda + k(k - k_2\alpha)$$

By using (19) and (20), it deduces that $A$ is Hurwitz. Solving (22) results in

$$\begin{bmatrix} e_1 \\ e_2 \end{bmatrix} = \mathrm{e}^{A(t-t_0)} \begin{bmatrix} e_1 \\ e_2 \end{bmatrix}_{t=t_0} - \int_{t_0}^{t} \mathrm{e}^{-A(t-\tau)} \begin{bmatrix} 0 \\ 1 \end{bmatrix} v_r \alpha \sin e_3 \mathrm{d}\tau$$

Because $v_r \to 0$, it yields $\forall \varepsilon > 0, \exists T > 0$, when $t \geqslant T$, $|v_r(t)| \leqslant \varepsilon$.

Set $t_0 = T$. Then

$$\begin{bmatrix} e_1(t) \\ e_2(t) \end{bmatrix} = \mathrm{e}^{A(t-T)} \begin{bmatrix} e_1 \\ e_2 \end{bmatrix}_{t=T} - \int_{T}^{t} \mathrm{e}^{A(t-\tau)} \begin{bmatrix} 0 \\ 1 \end{bmatrix} v_r \alpha \sin e_3 \mathrm{d}\tau$$

For the same $\varepsilon > 0$, $\exists \overline{T} > 0$ ($\overline{T} > 0$), when $t > \overline{T}$, it has

$$\left\| \mathrm{e}^{A(t-T)} \begin{bmatrix} e_1 \\ e_2 \end{bmatrix}_{t=T} \right\|_1 \leqslant \varepsilon$$

Hence

$$\begin{aligned} \left\| \begin{bmatrix} e_1 \\ e_2 \end{bmatrix} \right\|_1 &\leqslant \varepsilon + \alpha\varepsilon \left\| \int_T^t \mathrm{e}^{-A(t-\tau)} \begin{bmatrix} 0 \\ 1 \end{bmatrix} \mathrm{d}\tau \right\|_1 \\ &= \varepsilon + \alpha\varepsilon \left\| A^{-1}(I - \mathrm{e}^{-A(t-T)}) \begin{bmatrix} 0 \\ 1 \end{bmatrix} \right\|_1 \\ &\leqslant \varepsilon + \alpha\varepsilon \|A^{-1}\|_1 \end{aligned}$$

In addition,

$$A^{-1} = \begin{bmatrix} 0 & -\frac{1}{k} \\ \frac{1}{k - k_2\alpha} & -\frac{-k_1\alpha}{k(k - k_2\alpha)} \end{bmatrix}$$

$$\begin{aligned} \|A^{-1}\|_1 &\leqslant \max\left\{ \left|\frac{1}{k}\right|, \left|\frac{1}{k - k_2\alpha}\right| + \left|\frac{k_1\alpha}{k(k - k_2\alpha)}\right| \right\} \\ &\leqslant \max\left\{ \frac{1}{|k|}, \frac{1}{|k - k_2\overline{\alpha}|} + \frac{|k_1\overline{\alpha}|}{|k(k - k_2\overline{\alpha})|} \right\} \triangleq m \end{aligned}$$

where $m$ is a constant only dependent on $k, k_1, k_2, \underline{\alpha}$ and $\overline{\alpha}$. Therefore

$$|e_i| \leqslant \varepsilon + \varepsilon\alpha m = \varepsilon(1 + \alpha m), \quad i = 1, 2$$

When $t \geqslant \overline{T}$, go to next step.

**Step 2** The controller is defined as following

$$v = v_r \cos e_3 + k e_1, \omega_r - \omega = -k_3 e_3 - \frac{e_2 v_r \sin e_3}{e_3} \frac{e_3^2(\overline{T})}{\varepsilon}$$

where $k > 0, k_3 > 0$,which can be chosen arbitrarily.

The candidate Lyapunov function $V$ is chosen as following

$$V(t) = \frac{1}{2}\left( e_1^2 + e_2^2 + \alpha \frac{\varepsilon}{e_3^2(\overline{T})} e_3^2 \right)$$

The derivative of it with respective to $t$ is

$$\dot{V}(t) = -k\alpha e_1^2 - k_3\alpha \frac{\varepsilon}{e_3^2(\overline{T})} e_3^2$$

and

$$V(\overline{T}) \leqslant \frac{1}{2}(e_1^2(\overline{T}) + e_2^2(\overline{T}) + \overline{\alpha}\varepsilon)$$

Then $V(t)$ is decreasing. Therefore

$$\frac{1}{2} e_2^2(t)) \leqslant V(t) \leqslant V(\overline{T}), \quad t \geqslant \overline{T}$$

or

$$|e_2(t)| \leqslant \sqrt{2V(\overline{T})} \leqslant \sqrt{2\varepsilon(1 + \alpha m) + \overline{\alpha}\varepsilon}, \quad t \geqslant \overline{T}$$

Therefore the change of $e_2$ can be made small enough. By the same argument, $e_1$ and $e_3$ are convergent to zero as $t \to \infty$. Summing up, when $t$ is large enough, $e_1$, $e_2$ and $e_3$ can be made small enough as desired because $\varepsilon$ is arbitrarily given in advance.

## 4 SIMULATION

The simulation was implemented for the the controller defined in (16). The corresponding closed loop system was written by (18). The desired velocity was chosen as $v_r = 1.5$ m/s, $\omega_r = 0.4$ rad/s, $\alpha = 1.5$, $\theta_0 = 1.2$ rad. The parameters were chosen as $k_1 = 1, k_3 = 2$.

Take the initial value $[1.2, 0.4, 0.3]$ for the configuration of the desired robot. Choose the initial value $[0.2, 2.2, 0.6]$ for the configuration of the actual robot. The tracking trajectories of states and movements of the robot are shown in Fig.2~Fig.3, respectively.

In the simulation, as long as $k_1$ and $k_3$ were chosen positive, the errors were convergent. In the case, $k_1 = 1, k_2 = 2$, the result was better. When one of $k_1$ and $k_3$ were chosen negative, the convergence of the errors could not be guaranteed. Generally there were little effect caused by the change of $\alpha$ and $\theta_0$. In the similar way, the simulation for the second controller could be done. Here omitted due to limit space.

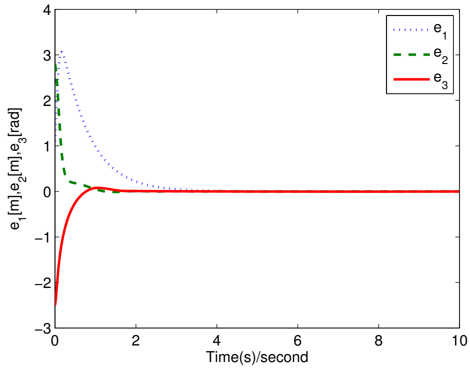


**Fig. 2 The trajectories of error state $e_1$, $e_2$ and $e_3$ in the image frame with respect to time**

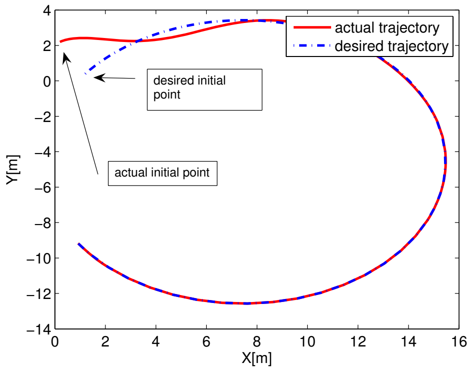


**Fig. 3 The tracking trajectories of the robot in the inertial frame with respect to the desired robot**

## 5 CONCLUSION

This paper investigated the visual servoing tracking of nonholonomic mobile robots. Barbalat theorem and two-step techniques were exploited to craft the robust controllers that enable the mobile robot image pose and the orientation tracking despite the lack of depth information and the lack of precise visual parameters. The most interesting feature of this paper is that the problem was discussed in the image frame and the inertial frame, which made the problem easy and useful. The convergence of the error system by using the proposed method was rigorously proved.

## REFERENCES


[1] Nakamura Y. Nonholonornic Robot Systems, Part 1- Parts. Journal of the JRSJ, 1993, 1994, 11(4-7); 12(2).

[2] Kolmanovsky I, McClamroch N H. Developments in Nonholonomic Control Problems. IEEE Control Systems Magazine, 1995, 15(6):20-36.

[3] Brockett R. Asymptotic Stability and Feedback Stabilization. Birkhauser, 1983.

[4] Murray R, Sastry S. Nonholonomic Motion Planning: Steering Using Sinusoids. IEEE Trans. on Automatic Control, 1993, 38:700-716.

[5] Sordalen O J, Egeland O. Exponential Stabilization of Nonholonomic Chained Systems. IEEE Automatic Control, 1995, 40(1):35-49.

[6] Jiang Z P, Nijmeijer H. Tracking Control of Mobile Robots: A Case Study in Backstepping. Automatica, 1997, 33(7):1393-1399.

[7] Aicardi M, Casaliio G, Balestrino A, Bicchi A. Closed Loop Smooth Steering of Unicycle-like Vehicles. Proc. CDC, 1994, 3:2455-2458.

[8] Allen P K, Timcenko A, Yoshimi B, Michelman P. Automated Tracking and Grasping of a Moving Object with a Robotic Hand-eye System. IEEE Trans. Robot. Automat., Apr. 1993, 9:152-165.

[9] Hutchinson S, Hager G D, Corke P L. Tutorial on visual servo control. IEEE Tram. Rob. Autom., 1996, 12(5):651-670.

[10] Hebert M. 3-D Vision for Outdoor Navigation by an Autonomous Vehicle. The Image Understanding Workshop, Cambridge, U.K., 1998.

[11] Kim B H, et al. Localization of a Mobile Robot Using Images of a Moving Target. Proc. IEEE Int. Conf. Robotics Automation, 2001:253-258.

[12] Dixon W E, Dawson D M, Zergeroglu E, Behal A. Adaptive Tracking Control of a Wheeled Mobile Robot via an Uncalibrated Camera System. Proc. IEEE American Control Conf., Chicago, IL, Jun. 2000:1493-1497.

[13] Wang H Y, Itani S, Fukao T, Adachi N. Image-Based Visual Adaptive Tracking Control of Nonholonomic Mobile Robots. Proc. IEEE/RJS Int. Conf. Intelligent Robots and Systems, 2001:1-6.

[14] Slotine J J E, Li Weiping. Applied Nonlinear Control. Englewood Cliffs, New Jersey: Prentice Hall, 1991.